Geophys. J. Int. (2005) **161,** 881–890 doi: 10.1111/j.1365-246X.2005.02581.x

Poroelastic fluid effects on shear for rocks with soft anisotropy

James G. Berryman

University of California, Lawrence Livermore National Laboratory, PO Box 808 L-200, *Livermore CA* 94551-9900, *USA*

Accepted 2005 January 10. Received 2005 January 4; in original form 2004 July 9

SUMMARY

A general analysis of poroelasticity for vertical transverse isotropy (VTI) shows that four eigenvectors are pure shear modes with no coupling to the pore-fluid mechanics. The remaining two eigenvectors are linear combinations of pure compression and uniaxial shear, both of which are coupled to the fluid mechanics. After reducing the problem to a 2×2 system, the analysis shows in a relatively elementary fashion how a poroelastic system with isotropic solid elastic frame, but with anisotropy introduced only through the poroelastic coefficients (and, therefore, termed soft anisotropy), interacts with the mechanics of the pore fluid and produces shear dependence on fluid properties in the overall poroelastic system. The analysis shows, for example, that this effect is always present (though sometimes small in magnitude) in the systems studied and can be comparatively large (on the order of 10 to 20 per cent) for wave propagation studies in some rocks, including Sierra White granite and Spirit River sandstone. Some of the results quoted here are obtained by using a new product formula relating local bulk and uniaxial shear energy to the product of the two eigenvalues that are coupled to the fluid mechanics. This product formula was first derived in prior work. The results obtained here are observed to be useful both for explaining difficult to reconcile laboratory wave propagation (especially ultrasonic) data showing that the shear modulus exhibits clear dependence on fluid content and also for benchmarking of poroelastic codes.

Key words: anisotropy, poroelasticity, shear deformation, solid–fluid interaction.

1 INTRODUCTION

Recent experimental results in ocean sediment acoustics (Williams *et al.* 2002) tend to show that there are significant discrepancies between Biot's theory (Biot 1962a,b) and measured poroelastic wave attenuation in the frequency band 2.6–400 kHz. The observed attenuation shows a different frequency dependence and greater overall reduction in wave amplitude than that predicted by the theory. Some plausible alternative theories have been proposed to reconcile these data, but so far none of these has been definitively determined to be the true source of the discrepancies. Similarly, a series of experiments on saturated sedimentary rocks by Sams *et al.* (1997) ranging from 30 Hz to 900 kHz has shown that the theory can be used to fit these seismic, well-logging and laboratory ultrasonic data. However, in order to do so, Biot's theory must be supplemented with some additional mechanisms to explain fully the poroelastic velocity dispersion and wave attenuation observed. Again the data available are not yet sufficient to help us distinguish with certainty what the precise cause of these significant variations of the data with frequency might be.

There have been many proposals made that supply physically reasonable mechanisms resulting in greater dispersion and attenuation in field data (see, for example, Pride *et al.* 2004, and references therein), but it is beyond our purpose and scope to review these here. The point to be made instead is that the measured effects are clearly multiscale phenomena and they are usually not treated as such (but see Pride *et al.* 2004, for one exception). Biot's theory is a relatively simple one for the complex systems considered. For fundamental reasons required to produce such a simple phenomenological theory, Biot necessarily assumed that the medium has constant porosity and is microhomogeneous, linear, usually isotropic, etc. Virtually all of these fundamental requirements of the theory are often violated in the earth for the applications of interest. Nevertheless, it is known that ultrasonic data (Plona 1980) on samples of sintered glass beads (and satisfying all Biot's assumptions) can be reconciled with the theory in detail (Chin *et al.* 1985; Bourbié *et al.* 1987), including wave speeds, attenuation and the predicted existence of a second compressional wave. So, it is the present author's working hypothesis that the underlying reason for many of the observed discrepancies in both laboratory, field and ocean sediment data, in all cases involving earth materials, is heterogeneity or anisotropy, or some combination of the two. If, for example, fluids affect the shear response of heterogeneous and anisotropic media at the microscale or mesoscale, then there is a high probability that field results, which are usually studied at the macroscale using isotropic models, will be misinterpreted. So it is important first to understand what effects should be expected and then later to produce properly upscaled equations that more accurately reflect the behaviour of these complex systems.

In recent papers (Berryman 2004a,c; 2005), the author has addressed the issue of heterogeneity for elastic or poroelastic media

in this context and shown how layering affects the overall shear modulus of such a system. An important outcome of the work (Berryman 2004a) was a rigorous product formula, valid for any transversely isotropic (hexagonal symmetry) poroelastic medium, and showing how the compressional and shear moduli are coupled under undrained conditions. Such undrained conditions are typically studied in poroelastic wave problems (see Hellmich & Ulm 2004, for a biomechanics example) as a proxy for the more difficult problem of understanding exactly how the system behaves at high frequencies, i.e. sufficiently high that the fluid is essentially confined (some authors, e.g. Mavko & Jizba 1991, use the term unrelaxed in this context) during the time of wave passage. We also study the undrained shear modulus in the present contribution, but no layering will be assumed: in order that we may separate out the contributions of heterogeneity from those of anisotropy. In fact, we find that the contributions from heterogeneity and anisotropy are very similar in these systems. This is a result in part, of course, of the fact that locally layered heterogeneity also leads to effective overall anisotropy.

A brief history of the theory on this topic is this: an important paper by Gassmann (1951) concerns the effects of fluids on the mechanical properties of porous rock. His main result is the well-known fluid-substitution formula (that now bears his name) for the bulk modulus in undrained, isotropic poroelastic media. He also postulated that the effective undrained shear modulus would (in contrast to the bulk modulus) be independent of the mechanical properties of the fluid when the medium is isotropic. That the independence of shear modulus from fluid effects is guaranteed for isotropic media at very low or quasi-static frequencies was shown recently by Berryman (1999) to be tightly coupled to the original bulk modulus result of Gassmann; each result implies the other in isotropic media. [Note that the recently discovered product formula (Berryman 2004a) suggests that there is also a similarly tight coupling between the modes for heterogeneous and anisotropic systems, as will be elaborated upon here.] It has gone mostly without discussion in the literature that Gassmann (1951) also derived general results for anisotropic porous rocks in the same 1951 paper. It is not hard to see that these results imply that, contrary to the isotropic case, some of the overall undrained (or, for ultrasonic data, some authors prefer the term unrelaxed) shear moduli in fact may depend on fluid properties in anisotropic media, thus mimicking the bulk modulus behaviour. However, Gassmann's paper does not remark at all on this difference in behaviour between isotropic and anisotropic porous rocks. Brown & Korringa (1975) also address the same class of problems, including both isotropic and anisotropic cases, but again they do not remark on the shear modulus results in either case. Norris (1993) studies partial saturation in isotropic layered materials in the low-frequency regime ($\simeq$100 Hz) and takes as a fundamental postulation that Gassmann's results hold for the low-frequency shear modulus, but it seems that some further justification should be provided for such an assumption and, furthermore, some indication of its range of validity established.

On the other hand, Hudson (1981), in his early work on cracked solids, explicitly demonstrates differences between fluid-saturated and dry cracks, and relates his work to that of Walsh (1969) and O'Connell & Budiansky (1974), but does not make any connection to the work of Gassmann (1951), Biot & Willis (1957), or Brown & Korringa (1975). Mukerji & Mavko (1994) show numerical results based on work of Gassmann (1951), Brown & Korringa (1975) and Hudson (1981) demonstrating the fluid dependence of shear in anisotropic rock, but again they do not remark on these results at all. Mavko & Jizba (1991) use a rather simple reciprocity argument within linear elasticity theory to establish a direct, but approximate, connection between undrained shear response and undrained compressional response in rocks containing very small volume cracks. Berryman & Wang (2001) show that deviations from Gassmann's results sufficient to produce shear modulus dependence on fluid mechanical properties require the presence of some anisotropy on the microscale, thereby explicitly violating the microhomogeneous and microisotropy conditions implicit in Gassmann's original derivation. Berryman *et al.* (2002a) go further and make use of differential effective medium analysis to show explicitly how the undrained, overall isotropic shear modulus can depend on fluid trapped in randomly oriented penny-shaped cracks. Meanwhile, laboratory results for wave propagation (see Berryman *et al.* 2002b) show conclusively that the shear modulus does indeed depend on fluid mechanical properties for low-porosity, low-permeability rocks and high-frequency laboratory experiments ($>$ 500 kHz).

One thing lacking from all the preceding work is a simple example showing how the presence of anisotropy influences the shear modulus, and specifically when and how the shear modulus becomes fluid-dependent. Our main purpose in the present work is therefore to demonstrate, in a set of (by design) quite elementary examples, how the overall shear behaviour becomes coupled to fluid compressional properties at high frequencies in anisotropic media: even though overall shear modulus is always independent of the fluid properties in microhomogeneous isotropic media at sufficiently low frequencies, whether drained or undrained. Two other distinct but related analyses addressing this topic have been presented recently by the author (Berryman 2004a,c). Both of these prior papers have made explicit use of layered media, composed of isotropic poroelastic materials, together with exact results for such media based on low-frequency, long-wavelength Backus averaging (Backus 1962). In contrast, the present analysis does not make use of such a specific model and is therefore believed to be about as simple as possible, while still achieving the level of understanding desired for this rather subtle technical issue. One important simplification we make here in order to separate the part that is the reuslt of poroelastic effects from whatever part would be present in any elastic (i.e. possibly zero permeability) porous medium is to model each material as if the elastic part is entirely isotropic, while the poroelastic effects [i.e. the effective stress or Biot–Willis coefficients (Biot & Willis 1957) for the anisotropic overall material] provide the only sources of anisotropy in the system. Thus, we specifically distinguish two possible sources of anisotropy, the elastic or hard anisotropy that is assumed not to be present here and the poroelastic or soft anisotropy (presumably introduced by complex pore shapes and non-uniform pore orientations) that is the only source of the effects we want to study in the present paper.

Our analysis for general transversely isotropic media is presented in Sections 2–4. To be specific, Section 4 also introduces the effective undrained shear modulus relevant to the general discussion. Examples are presented for granite and sandstone in Section 5. The results and conclusions of the paper are summarized in the final section. Some mathematical details are collected in two Appendices.

2 FLUID-SATURATED POROELASTIC ROCKS

In contrast to traditional elastic analysis, the presence in rock of a saturating pore fluid introduces the possibility of an additional control field and an additional type of strain variable. The pressure p_f in the fluid is a new field parameter that can be controlled. Allowing sufficient time for global pressure equilibration permits us to

consider p_f to be a constant throughout the percolating (connected) pore fluid, while restricting the analysis to quasi-static processes. (However, ultimately we are not interested in such quasi-static processes in this paper, as we are trying to reconcile laboratory wave data with the theory.) The change ζ in the amount of fluid mass contained in the pores (see Biot 1962a,b, or Berryman & Thigpen 1985) is a new type of strain variable, measuring how much of the original fluid in the pores is squeezed out during the compression of the pore volume while including the effects of compression or expansion of the pore fluid itself as a result of changes in p_f. It is most convenient to write the resulting equations in terms of compliances rather than stiffnesses, so the basic equation to be considered takes the following form for isotropic media:

$$\begin{pmatrix} e_{11} \\ e_{22} \\ e_{33} \\ -\zeta \end{pmatrix} = \begin{pmatrix} s_{11} & s_{12} & s_{12} & -\beta \\ s_{12} & s_{11} & s_{12} & -\beta \\ s_{12} & s_{12} & s_{11} & -\beta \\ -\beta & -\beta & -\beta & \gamma \end{pmatrix} \begin{pmatrix} \sigma_{11} \\ \sigma_{22} \\ \sigma_{33} \\ -p_f \end{pmatrix}. \tag{1}$$

The constants appearing in the matrix on the right-hand side will be defined in the following two paragraphs. It is important to write the equations this way rather than using the inverse relation in terms of the stiffnesses, because the compliances s_{ij} appearing in eq. (1) are simply related to the drained elastic constants λ_{dr} and G_{dr} in the same way they are related in normal elasticity, whereas the individual stiffnesses obtained by inverting the equation in eq. (1) must contain coupling terms through the parameters β and γ that depend on the pore and fluid compliances. Thus, we find that

$$s_{11} = \frac{1}{E_{dr}} = \frac{\lambda_{dr} + G_{dr}}{G_{dr}(3\lambda_{dr} + 2G_{dr})} \tag{2}$$

and

$$s_{12} = -\frac{\nu_{dr}}{E_{dr}}, \tag{3}$$

where the drained Young's modulus E_{dr} is defined by the second equality of eq. (2) and the drained Poisson's ratio is determined by

$$\nu_{dr} = \frac{\lambda_{dr}}{2(\lambda_{dr} + G_{dr})}. \tag{4}$$

When the external stress is hydrostatic so $\sigma = \sigma_{11} = \sigma_{22} = \sigma_{33}$, eq. (1) telescopes down to

$$\begin{pmatrix} e \\ -\zeta \end{pmatrix} = \begin{pmatrix} 1/K_{dr} & -\alpha/K_{dr} \\ -\alpha/K_{dr} & \alpha/BK_{dr} \end{pmatrix} \begin{pmatrix} \sigma \\ -p_f \end{pmatrix}, \tag{5}$$

where $e = e_{11} + e_{22} + e_{33}$, $K_{dr} = \lambda_{dr} + \frac{2}{3}G_{dr}$ is the drained bulk modulus, $\alpha = 1 - K_{dr}/K_m$ is the Biot–Willis parameter (Biot & Willis 1957), with K_m being the bulk modulus of the solid minerals present, and Skempton's pore-pressure build-up parameter B (Skempton 1954) is given by

$$B = \frac{1}{1 + K_p(1/K_f - 1/K_m)}. \tag{6}$$

New parameters appearing in eq. (6) are the bulk modulus of the pore fluid K_f and the pore modulus $K_p^{-1} = \alpha/\phi K_{dr}$, where ϕ is the porosity. The expressions for α and B can be generalized slightly by supposing that the solid frame is composed of more than one constituent, in which case the K_m appearing in the definition of α is replaced by K_s and the K_m appearing explicitly in eq. (6) is replaced by K_ϕ (see Brown & Korringa 1975; Rice & Cleary 1976; Berryman & Wang 1995). This is an important additional complication (Berge & Berryman 1995), but (for the sake of desired simplicity) we will not pursue the matter further here.

Comparing eqs (1) and (5), we find that

$$\beta = \frac{\alpha}{3K_{dr}} \tag{7}$$

and

$$\gamma = \frac{\alpha}{BK_{dr}}. \tag{8}$$

As we develop the ideas to be presented here, we will need to treat eqs (1)–(6) as if they are true locally, but perhaps not globally. In particular, if we assume overall drained conditions, then $p_f =$ a constant everywhere. However, if we assume locally undrained conditions, then $p_f \simeq$ a constant in local patches, therefore these locally constant values may differ from patch to patch. This way of viewing the system is intended to mimic the behaviour expected when a high-frequency wave propagates through a system having either highly variable, or just uniformly very low, fluid permeability everywhere.

3 RELATIONS FOR ANISOTROPY IN POROELASTIC MATERIALS

Gassmann (1951), Brown & Korringa (1975) and others have considered the problem of obtaining effective constants for anisotropic poroelastic materials when the pore fluid is confined within the pores. The confinement condition amounts to a constraint that the increment of fluid content $\zeta = 0$, while the external loading σ is changed and the pore-fluid pressure p_f is allowed to respond as necessary and thus equilibrate.

To provide an elementary derivation of the Gassmann equation for anisotropic materials, we consider the anisotropic generalization of eq. (1):

$$\begin{pmatrix} e_{11} \\ e_{22} \\ e_{33} \\ -\zeta \end{pmatrix} = \begin{pmatrix} s_{11} & s_{12} & s_{13} & -\beta_1 \\ s_{12} & s_{22} & s_{23} & -\beta_2 \\ s_{13} & s_{23} & s_{33} & -\beta_3 \\ -\beta_1 & -\beta_2 & -\beta_3 & \gamma \end{pmatrix} \begin{pmatrix} \sigma_{11} \\ \sigma_{22} \\ \sigma_{33} \\ -p_f \end{pmatrix}. \tag{9}$$

Three shear contributions have been excluded from consideration because they can easily be shown not to interact mechanically with the fluid effects. This form is not completely general in that it includes orthorhombic, cubic, hexagonal and all isotropic systems, but excludes triclinic, monoclinic, trigonal and some tetragonal systems that would have some non-zero off-diagonal terms in the full elastic matrix. Also, we have assumed that the material axes are aligned with the spatial axes. However, this latter assumption is not significant for the derivation that follows. Such an assumption is important when properties of laminated materials having arbitrary orientation relative to the spatial axes need to be considered, but we do not treat this more general problem here.

If the fluid is confined (or undrained on the timescales of interest), then $\zeta \equiv 0$ in eq. (9) and p_f becomes a linear function of σ_{11}, σ_{22}, σ_{33}. Eliminating p_f from the resulting equations, we obtain the general expression for the strain dependence on external stress under confined conditions:

$$\begin{aligned} \begin{pmatrix} e_{11} \\ e_{22} \\ e_{33} \end{pmatrix} &= \left[\begin{pmatrix} s_{11} & s_{12} & s_{13} \\ s_{12} & s_{22} & s_{23} \\ s_{13} & s_{23} & s_{33} \end{pmatrix} - \gamma^{-1} \begin{pmatrix} \beta_1 \\ \beta_2 \\ \beta_3 \end{pmatrix} (\beta_1 \ \beta_2 \ \beta_3) \right] \begin{pmatrix} \sigma_{11} \\ \sigma_{22} \\ \sigma_{33} \end{pmatrix} \\ &\equiv \begin{pmatrix} s^*_{11} & s^*_{12} & s^*_{13} \\ s^*_{12} & s^*_{22} & s^*_{23} \\ s^*_{13} & s^*_{23} & s^*_{33} \end{pmatrix} \begin{pmatrix} \sigma_{11} \\ \sigma_{22} \\ \sigma_{33} \end{pmatrix}. \end{aligned} \tag{10}$$

The s_{ij} are fluid-drained constants, while the s^*_{ij} are the fluid-undrained (or fluid-confined) constants.

The fundamental result (10) was obtained earlier by both Gassmann (1951) and Brown & Korringa (1975), and may be written simply as

$$s^*_{ij} = s_{ij} - \frac{\beta_i \beta_j}{\gamma}, \quad \text{for} \quad i, j = 1, 2, 3. \tag{11}$$

This expression is just the anisotropic generalization of the well-known Gassmann equation for isotropic, microhomogeneous porous media.

4 EIGENVECTORS FOR TRANSVERSE ISOTROPY

The 3×3 system (10) can be analysed fairly easily, and in particular the eigenfunctions and eigenvalues of this system can be obtained in general. However, such general results do not provide much physical insight into the problem we are trying to study, so instead of proceeding in this direction we will now restrict attention to transversely isotropic materials. This case is relevant to many layered earth materials and also industrial systems, and it is convenient because we can immediately eliminate one of the eigenvectors from further consideration. Three mutually orthogonal (but unnormalized) vectors of interest are

$$v_1 = \begin{pmatrix} 1 \\ 1 \\ 1 \end{pmatrix}, \qquad v_2 = \begin{pmatrix} 1 \\ -1 \\ 0 \end{pmatrix}, \qquad v_3 = \begin{pmatrix} 1 \\ 1 \\ -2 \end{pmatrix}. \tag{12}$$

Treating these vectors as stresses, the first corresponds to a simple hydrostatic stress, the second to a planar shear stress and the third to a pure shear stress applied uniaxially along the z-axis (which would also be the symmetry axis for a layered system, but we are not treating such layered systems here). The relationship of these vectors to the standard triaxial testing scenario used in rock and soil mechanics is discussed in Appendix A.

Transverse isotropy of the layered system requires $s_{11} = s_{22}$, $s_{13} = s_{23}$ and, for the poroelastic problem, $\beta_1 = \beta_2$. Thus, it is immediately apparent that the planar shear stress v_2 is an eigenvector of the system and, furthermore, it results in no contribution from the pore fluid. Therefore, this vector will be of no further interest here and the system can thereby be reduced to 2×2.

4.1 Compliance formulation

If we define the effective compliance matrix for the system as S^* having the matrix elements given in eq. (11), then the bulk modulus for this system is defined in terms of v_1 by

$$\frac{1}{K_u} = v_1^T S^* v_1 = \frac{1}{K_{dr}} - \gamma^{-1} (2\beta_1 + \beta_3)^2, \tag{13}$$

where the T superscript indicates the transpose and $1/K_{dr} \equiv \sum_{i,j=1}^{3} s_{ij}$. This is the result usually quoted as Gassmann's equation for the bulk modulus of the undrained (or confined) anisotropic (vertical transverse isotropy, VTI) system. Also, note that in general

$$\sum_{i=1}^{3} \beta_i = 2\beta_1 + \beta_3 = \alpha / K_{dr}. \tag{14}$$

Thus, even though v_1 is not an eigenvector of this system, it nevertheless plays a fundamental role in the poromechanics. Furthermore, this role is quite well understood. What is perhaps not as well understood then, especially for poroelastic systems, is the role of v_3. Understanding this role will be one main focus for the remainder of this discussion.

The true eigenvectors of the subproblem of interest (i.e. in the space orthogonal to the four pure shear eigenvectors already discussed) are necessarily linear combinations of v_1 and v_3. We can construct the relevant contracted operator for the 2×2 subsystem by considering

$$\begin{pmatrix} v_1^T \\ v_3^T \end{pmatrix} S^* \begin{pmatrix} v_1 & v_3 \end{pmatrix} \equiv \begin{pmatrix} 9A^*_{11} & 18A^*_{13} \\ 18A^*_{13} & 36A^*_{33} \end{pmatrix} \tag{15}$$

(in all cases the * superscripts indicate that the pore-fluid effects are included) and the reduced matrix

$$\Sigma^* = A^*_{11} v_1 v_1^T + A^*_{13} \left(v_1 v_3^T + v_3 v_1^T \right) + A^*_{33} v_3 v_3^T, \tag{16}$$

where

$$\begin{aligned} A^*_{11} &= \left[2\left(s^*_{11} + s^*_{12} + 2s^*_{13} \right) + s^*_{33} \right] / 9, \\ A^*_{13} &= \left(s^*_{11} + s^*_{12} - s^*_{13} - s^*_{33} \right) / 9, \\ A^*_{33} &= \left(s^*_{11} + s^*_{12} - 4s^*_{13} + 2s^*_{33} \right) / 18 . \end{aligned} \tag{17}$$

Providing some understanding of these connections and the implications for shear modulus dependence on fluid content is one of our goals.

First, we remark that $A^*_{11} = 1/9K_u$, where K_u is again the undrained (or Gassmann) bulk modulus for the system in eq. (13). Therefore, A^*_{11} is proportional to the undrained bulk compliance of this system. The other two matrix elements cannot be given such simple interpretations in general. To simplify the analysis somewhat further we note that, at least for purposes of modeling, anisotropy of the compliances s_{ij} and the poroelastic coefficients β_i can be treated independently. Anisotropy displayed in the s_{ij} corresponds mostly to the anisotropy in the solid elastic components of the system, while anisotropy in the β_i corresponds mostly to anisotropy in the shapes and spatial distribution and orientation of the porosity. We will therefore distinguish these contributions by calling anisotropy appearing in the s_{ij} the hard anisotropy and the anisotropy in the β_i will in contrast be called the soft anisotropy.

Now, it is clear (also see the discussion in Appendix B for more details) that the eigenvectors having unit magnitude $f(\theta)$ for this problem (i.e. for the reduced operator Σ^*) necessarily take the form

$$f(\theta) = \overline{v}_1 \cos\theta + \overline{v}_3 \sin\theta, \tag{18}$$

where $\overline{v}_1 = v_1/\sqrt{3}$ and $\overline{v}_3 = v_3/\sqrt{6}$ are the normalized basis vectors. The 2×2 system must have two eigenvectors, corresponding to two angles we label θ_+ and θ_- (for the $\pm$ signs appearing in the quadratic forms that appear in the eigenvalue formulae). Furthermore, the orthogonality condition for the eigenvectors is

$$0 = f^T(\theta_+) f(\theta_-) = \cos\theta_+ \cos\theta_- + \sin\theta_+ \sin\theta_- = \cos(\theta_+ - \theta_-), \tag{19}$$

which implies that the difference $\theta_+ - \theta_- = \pm\pi/2$. The two solutions for the rotation angle, when chosen appropriately, may therefore be related by θ_+ and $\theta_- = \theta_+ + \frac{\pi}{2}$. It is easily seen that the eigenvalues are given by

$$\Lambda^*_{\pm} = 3\left[A^*_{33} + A^*_{11}/2 \pm \sqrt{\left(A^*_{33} - A^*_{11}/2 \right)^2 + 2\left(A^*_{13} \right)^2} \right] \tag{20}$$

and the rotation angles are determined by

$$\begin{aligned} \tan\theta^*_{\pm} &= \frac{\Lambda^*_{\pm}/3 - A^*_{11}}{\sqrt{2} A^*_{13}} \\ &= \frac{\left[A^*_{33} - A^*_{11}/2 \pm \sqrt{\left(A^*_{33} - A^*_{11}/2 \right)^2 + 2(A^*_{13})^2} \right]}{\sqrt{2} A^*_{13}}. \end{aligned} \tag{21}$$

One part of the rotation angle is the result of the drained (fluid free) hard anisotropic nature of the rock frame material. We will call this part $\bar{\theta}$. The remainder is the result of the presence of the fluid in the pores and we will call this part $\delta\theta \equiv \theta^* - \bar{\theta}$ for the soft anisotropy. Using a standard formula for tangents, we have

$$\delta\theta_\pm = \tan^{-1}\left(\frac{\tan\theta^*_\pm - \tan\bar{\theta}_\pm}{1 + \tan\theta^*_\pm \tan\bar{\theta}_\pm}\right). \tag{22}$$

Furthermore, definite formulae for $\bar{\theta}_\pm$ are found from eq. (21) by taking $\gamma \to \infty$ (corresponding to air saturation of the pores).

Because eq. (19) implies that

$$\tan\theta^*_+ \cdot \tan\theta^*_- = -1, \tag{23}$$

it is sufficient to consider just one of the signs in front of the radical in eq. (21). The most convenient choice for analytical purposes turns out to be the minus sign (which corresponds to the eigenvector with the larger component of pure compression). Furthermore, it is also clear from the form of eq. (21) that often the behaviour of most interest to us here occurs for cases when $A^*_{13} \neq 0$.

In the limit of a nearly isotropic solid frame (so the hard anisotropy vanishes and thus we will also call this the quasi-isotropic limit), it is not hard to see that

$$A^*_{33} \simeq \frac{1}{12G_{\rm dr}} - \frac{(\beta_1 - \beta_3)^2}{9\gamma}, \tag{24}$$

where $G_{\rm dr}$ is the drained shear modulus of the quasi-isotropic solid frame. Similarly, the remaining coefficient

$$A^*_{13} \simeq -\frac{(\beta_1 - \beta_3)(2\beta_1 + \beta_3)}{9\gamma}, \tag{25}$$

because all the solid contributions approximately cancel in this limit.

To clarify the situation further, we enumerate three cases, which follow.

4.1.1 Case I: $A^*_{33} - A^*_{11}/2 \neq 0$, $A^*_{13} = 0$

Whenever $A^*_{33} - A^*_{11}/2 \neq 0$ and $A^*_{13} \to 0$, we find easily $\theta^*_- \to 0$, while $\theta^*_+ \to \pi/2$. In this case, v_1 and v_3 are themselves the eigenvectors, while the eigenvalues are proportional to A^*_{11} and A^*_{33}. In the quasi-isotropic limit, A^*_{13} can vanish only if $\beta_1 - \beta_3 = 0$, in which case A^*_{33} also does not depend on fluid properties. For media differing significantly from the quasi-isotropic limit, A^*_{13} could vanish for some physically interesting situations, but the resulting physical constraints are too special (and complicated) for us to consider them further here.

4.1.2 Case II: $A^*_{33} - A^*_{11}/2 = 0$, $A^*_{13} \neq 0$

For this case, $\tan\theta^*_\pm = \pm 1$, so $\theta^*_\pm = \pm\pi/4$. The two eigenvectors are $v_1/\sqrt{6} \pm v_3/\sqrt{12}$, with no dependence on the fluid properties. However, the eigenvalues continue to be functions of the fluid properties. This seems to be a rather special case, but again considering the quasi-isotropic limit, we find that $A^*_{33} - A^*_{11}/2 \simeq \nu/2E + [(2\beta_1 + \beta_3)^2 - 2(\beta_1 - \beta_3)^2]/18\gamma$, where ν is Poisson's ratio and E is Young's modulus. For this combination of the parameters to vanish for special values does not appear to violate any of the well-known constraints (such as positivity, etc.) on these parameters. For example, if $\beta_1 = 0$, the term depending on the fluid properties clearly makes a negative contribution, which might be large enough to cancel the contribution from the solid. However, for now, this case seems rather artificial, so we will not consider it further here.

4.1.3 Case III: $A^*_{33} - A^*_{11}/2 \neq 0$, $A^*_{13} \neq 0$

This case is the most general one of the three and the one we will study at greater length in the remainder of this discussion.

We want to understand how the introduction of liquid into the pore space affects the shear modulus. We also want to know how the anisotropy influences, i.e. aids or hinders, the impact of the liquid on the shear behaviour. To achieve this understanding, it should be sufficient to consider the case when $(A^*_{13})^2 \ll (A^*_{33} - A^*_{11}/2)^2$, assuming as we do that both factors are non-zero. Then, expanding the square root in eq. (20), we have

$$\Lambda^*_+ = 6A^*_{33} + \Delta \quad \text{and} \quad \Lambda^*_- = 3A^*_{11} - \Delta, \tag{26}$$

where Δ is defined consistently by either of the two preceeding expressions or by $2\Delta \equiv \Lambda^*_+ - \Lambda^*_- + 3A_{11} - 6A_{33}$ and is also given approximately for cases of interest here by

$$\Delta \simeq \frac{3\left(A^*_{13}\right)^2}{A^*_{33} - A^*_{11}/2}. \tag{27}$$

In the quasi-isotropic soft anisotropy limit under consideration, we find

$$\Delta \simeq \frac{2(\beta_1 - \beta_3)^2(2\beta_1 + \beta_3)^2/27\gamma^2}{\nu/E + \left[(2\beta_1 + \beta_3)^2 - 2(\beta_1 - \beta_3)^2\right]/9\gamma}. \tag{28}$$

All of the mechanical effects of the liquid that contribute to this formula appear in the factor γ. The order at which γ appears depends on the relative importance of the two terms in the denominator of this expression. If the second term ever dominates, then one factor of γ cancels and therefore $\Delta \sim O(\gamma^{-1})$, and furthermore $\Delta \sim 2(\beta_1 - \beta_3)^2/3\gamma$ if $|\beta_1 - \beta_3| \ll |2\beta_1 + \beta_3|$. If what seems to be the more likely situation holds, then instead the first term in the denominator dominates and $\Delta \sim O(\gamma^{-2})$. So in either of these cases, as long as $\beta_1 - \beta_3 \neq 0$ (which is the condition for soft anisotropy), we always have contributions to Δ from liquid mechanical effects. There do not appear to be any combinations of the parameters for which the fluid effects disappear whenever the material is in the class of anisotropic solids considered here.

4.2 Stiffness formulation

The dual to the problem just studied replaces compliances everywhere with stiffnesses and then proceeds as before. Eqs (15)–(18) are replaced by

$$\begin{pmatrix} v_1^T \\ v_3^T \end{pmatrix} C^* \begin{pmatrix} v_1 & v_3 \end{pmatrix} \equiv \begin{pmatrix} 9B^*_{11} & 18B^*_{13} \\ 18B^*_{13} & 36B^*_{33} \end{pmatrix} \tag{29}$$

(in all cases the * superscripts indicate that the pore-fluid effects are included) and the reduced matrix

$$(\Sigma^*)^{-1} = B^*_{11} v_1 v_1^T + B^*_{13}\left(v_1 v_3^T + v_3 v_1^T\right) + B^*_{33} v_3 v_3^T, \tag{30}$$

where

$$\begin{aligned} B^*_{11} &= \left[2\left(c^*_{11} + c^*_{12} + 2c^*_{13}\right) + c^*_{33}\right]/9, \\ B^*_{13} &= \left(c^*_{11} + c^*_{12} - c^*_{13} - c^*_{33}\right)/9, \\ B^*_{33} &= \left(c^*_{11} + c^*_{12} - 4c^*_{13} + 2c^*_{33}\right)/18\,. \end{aligned} \tag{31}$$

It is a straightforward exercise to check that the two reduced problems are in fact inverses of each other. We will not repeat this analysis here, as it is wholly repetitive of what has gone before. The main difference in the details is that the expressions for the Bs in terms of the βs are rather more complicated than those for the compliance version, which is also why we chose to display the compliance formulation instead.

4.3 Effective and undrained shear moduli $G_{\rm eff}$ and $G_{\rm u}$

Four out of five shear moduli are easily defined for the anisotropic system under study. Furthermore, because we are treating only soft anisotropy, all of these moduli are the same, i.e. $G_i = G_{\rm dr}$ for $i = 1, \ldots, 4$. They are related to the four shear eigenvalues/eigenvectors of the system and they do not couple to the pore-fluid mechanics. However, the eigenvectors in the reduced 2×2 system studied here are usually mixed in character, being quasi-compressional or quasi-shear modes. It is therefore somewhat problematic to find a proper definition for a fifth shear modulus. The author has analysed this problem previously (Berryman 2004b) and concluded that a sensible (though approximate) definition can be made using $G_5 = G_{\rm eff}$. There are several different ways of arriving at the same result, but for the present analysis the most useful of these is to express $G_{\rm eff}$ in terms of the product $\Lambda_+\Lambda_-$ (the eigenvalue product, which is also the determinant of the 2×2 compliance system). For our present application, this result states that the product formula is

$$\frac{1}{3K_{\rm u}} \cdot \frac{1}{2G_{\rm eff}} \equiv \Lambda_+\Lambda_- = 18\left[A^*_{11}A^*_{33} - \left(A^*_{13}\right)^2\right], \tag{32}$$

which we take as the definition of $G_{\rm eff}$. Also, because $A^*_{11} = 1/9K_{\rm u}$, we have

$$\frac{1}{G_{\rm eff}} = 12\left[A^*_{33} - \left(A^*_{13}\right)^2/A^*_{11}\right]. \tag{33}$$

To obtain one possible choice for an estimate of the isotropic average overall undrained shear modulus, we next take the arithmetic mean of these five shear compliances:

$$\frac{1}{G_{\rm u}} \equiv \frac{1}{5}\sum_{i=1}^{5}\frac{1}{G_i}. \tag{34}$$

Combining these definitions and results gives

$$\frac{1}{G_{\rm u}} - \frac{1}{G_{\rm dr}} = -\frac{4}{15}\frac{(\beta'_1 - \beta'_3)^2}{1-\alpha B}\frac{\alpha B}{K_{\rm dr}} = \frac{4}{15}\frac{(\beta'_1 - \beta'_3)^2}{1-\alpha B}\left(\frac{1}{K_{\rm u}} - \frac{1}{K_{\rm dr}}\right), \tag{35}$$

where the βs are defined by $\beta'_i = \beta_i K_{\rm dr}/\alpha$. The final equality is presented to emphasize the similarity of the present results to those of both Mavko & Jizba (1991) and Berryman *et al.* (2002b). Setting $\beta'_1 = 0$, $\beta'_3 = 1$, $B = 1$ and $\alpha \simeq 0$ recovers the form of Mavko & Jizba (1991) for the case of a very dilute system of flat cracks. The Mavko–Jizba form was used successfully by Sams *et al.* (1997) while reconciling their high-frequency data with the theory.

Note that eq. (34) takes the form of a Reuss-type average (harmonic mean and lower bound) of the undrained shear modulus. Also note that, contrary to eq. (34), the definition (33) of $G_{\rm eff}$ is actually based instead on the Voigt average. In terms of mathematical precision, the result (35) therefore cannot be considered strictly rigorous; it is neither an upper nor a lower bound. A partial justification for the formula comes not from absolute rigour, but instead from observations (some of which are presented in the next section) that $G_{\rm eff}$ is in fact a very close estimate of the energy per unit volume in the fifth shear mode (though still an upper bound). So, for these reasons, the result (35) should be viewed, not as a rigorous formula (it is not), but as a good physical estimate of the undrained shear modulus. Berryman *et al.* (2002b) show that the Mavko & Jizba (1991) results suffer from the same lack of rigour.

For applications in which rigour is demanded, we should instead use the Voigt average

$$G_{\rm u} \equiv \frac{1}{5}\sum_i G_i \tag{36}$$

as our estimate of the effective undrained shear modulus. Berryman (2004a) shows that this choice is often a very accurate estimate, although strictly speaking it should still be viewed as an upper bound on the overall modulus for a random, heterogeneous and anisotropic system.

5 EXAMPLES AND DISCUSSION

It is clear from eq. (26) that fluid effects in Δ cannot increase the overall compliance eigenvalues simultaneously for both the quasi-bulk and the quasi-shear modes. Rather, if one increases, the other must decrease. Furthermore, it is certainly always true that the presence of pore liquid either has no effect or else strengthens (i.e. stiffens) the porous medium in compression. However, this effect on the bulk modulus has been at least partially accounted for in $A^*_{11} = 1/9K^*$ through the original contribution derived by Gassmann (1951). So presumably the contribution of Δ to compliance cannot be so large as to negate completely the liquid effects on the undrained bulk modulus.

5.1 Examples

To clarify the situation, we show some examples in Figs 1–4. The details of the analysis that produces these constant energy ellipses are summarized in Appendix B. The main point is that, for the compliance version of the analysis, the contours of constant energy are ellipses when the vector f in eq. (18) is interpreted as a stress. Analogously, when the vector is treated as a strain, the contours of constant energy are ellipses for the dual (or stiffness) formulation. If we choose to think of these figures as diagrams in the complex plane, then we note that, while circles and lines transform to circles and lines when transforming back and forth between these two planes, the shapes of ellipses are not preserved (except, of course, in the special case, which is precisely that of isotropy, when the ellipses

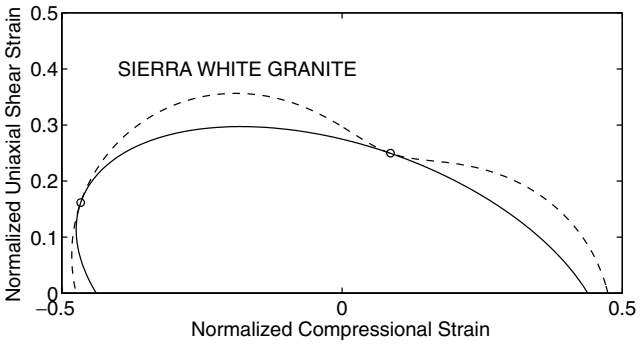

Figure 1. For Sierra White granite using the parameters from Table 1, the locus of points $z = Re^{i\theta}$ (see eq. A2) having constant energy, when the linear combination of pure compression and pure uniaxial shear is interpreted as a strain field applied to the stiffness matrix (solid line). The plot is in the complex z plane, with the inverse of the corresponding expression for the compliance energy superposed for comparison (dashed line). Circles at the two points of intersection correspond to the two eigenvalues/eigenvectors of the system of equations. The ellipse (solid curved line) in this plane corresponds to the more complex curve in Fig. 2.

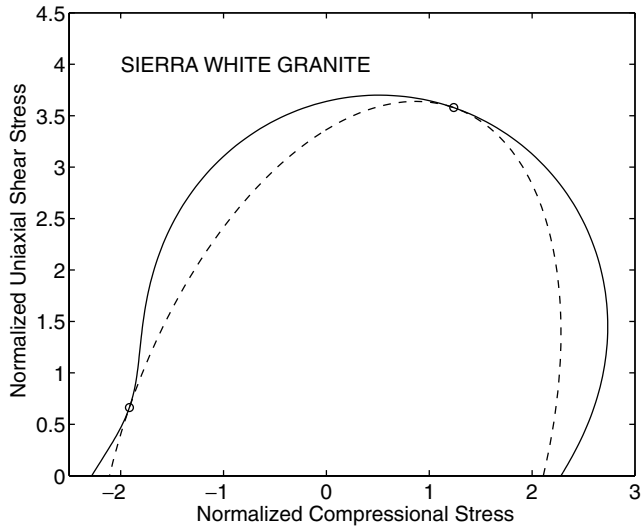

Figure 2. Same parameters as Fig. 1, but the linear combination of pure compression and pure uniaxial shear is interpreted as a stress field and is applied to the compliance matrix (dashed line). The plot is again in the complex z plane, with the inverse of the corresponding expression for the stiffness energy superposed for comparison (solid line). Circles at the two points of intersection correspond to the two eigenvalues/eigenvectors of the system of equations. The ellipse (dashed line) corresponds to the more complex curve in Fig. 1.

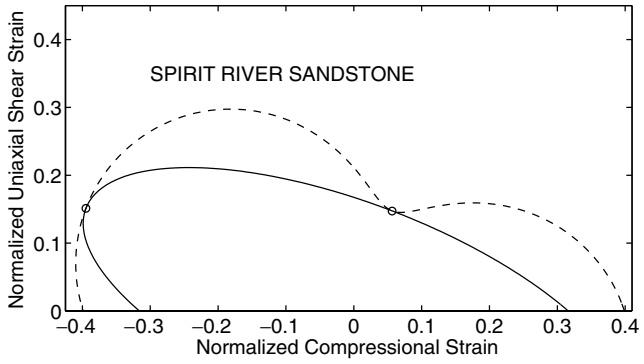

Figure 3. Same as Fig. 1 for Spirit River sandstone using the parameters from the Table 1.

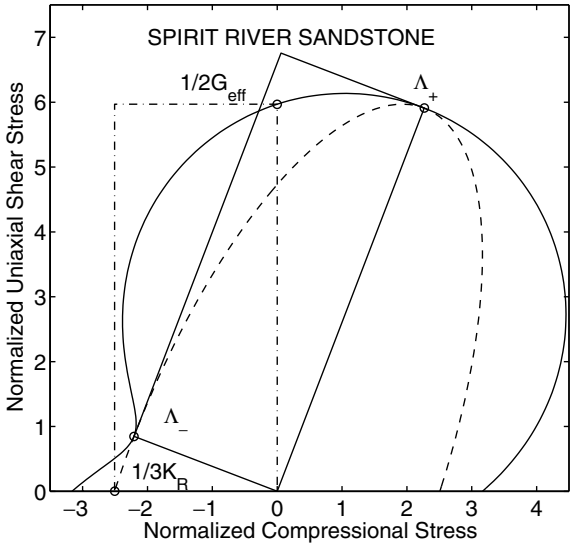

Figure 4. Same as Fig. 2 for Spirit River sandstone using the parameters from the Table 1. The two rectangles illustrate the product formula (32) derived and used in the text. The shapes of these rectangles, although very similar, are not identical; however, their areas are identical.

Table 1. Elastic and poroelastic parameters of the two rock samples considered in the text. Bulk and shear moduli of the grains K_m and G_m, bulk and shear moduli of the drained porous frame K_{dr} and G_{dr}, the effective and undrained shear moduli G_{eff} and G_u, and the Biot–Willis parameter $\alpha = 1 - K_{dr}/K_m$. The porosity is ϕ.

Elastic and poroelastic parameters	Sierra White granite	Spirit River sandstone
G_m (GPa)	31.7	69.0
G_u (GPa)	28.3	12.41
G_{dr} (GPa)	26.4	11.33
G_{eff} (GPa)	39.8	20.11
K_m (GPa)	57.7	30.0
K_{dr} (GPa)	38.3	7.04
α	0.336	0.765
ϕ	0.008	0.052

degenerate to circles). Eigenvectors are determined by the directions in which the points of contact of these two curves lie (indicated by small circles).

For the two sets of examples, the values used for the moduli of the samples are taken from results contained in Berryman (2004a), wherein it was shown how certain laboratory data could be fit using an elastic differential effective medium scheme. These results are summarized in the Table 1.

Figs 1 and 2 present results for Sierra White granite. Laboratory data on this material were presented by Murphy (1982). The values chosen for β_1 and β_3 were $\beta_1 = 0.05\alpha/K_{dr}$ and $\beta_3 = 0.90\alpha/K_{dr}$. The value of the energy used for normalization was $U \simeq 900.0$ GPa. Computed values for the effective and undrained shear moduli were $G_{eff} = 39.8$ GPa and $G_u = 28.3$ GPa.

Figs 3 and 4 present results for Spirit River sandstone. Laboratory data on this material were presented by Knight & Nolen-Hoeksema (1990). The values chosen for β_1 and β_3 were $\beta_1 = 0.25\alpha/K_{dr}$ and $\beta_3 = 0.50\alpha/K_{dr}$. The value of the energy used for normalization was $U \simeq 900.0$ GPa. Computed values for the effective and undrained shear moduli were $G_{eff} = 20.11$ GPa and $G_u = 12.41$ GPa.

5.2 Discussion

We can compare the results obtained with results obtained for the same rocks using differential effective medium theory to fit data. The two characteristics that will interest us here are: (i) comparisons between the values chosen in our examples for the anisotropic β and the best-fitting crack aspect ratios found in Berryman (2004a); and (ii) comparisons between the magnitudes of changes in the overall shear moduli from their drained to undrained values.

The preferred crack aspect ratios found for Sierra White granite and Spirit River sandstone in Berryman (2004a) were 0.005 and 0.0125, respectively. Here, we found that (β_1', β_3') for the same samples were (0.05, 0.90) and (0.25, 0.50), respectively. Clearly, these

values are at least weakly correlated with those of the aspect ratios for the same samples, but no stronger conclusions can be reached at the present time concerning these values.

Similarly, the comparisons of the changes in shear modulus magnitude from drained to undrained also show a weak correlation. The increases in shear moduli observed in the measured laboratory data for Sierra White granite and Spirit River sandstone are approximately 10 and 20 per cent, respectively. As seen in Table 1, the magnitude of the changes predicted here is essentially approximately 10 per cent in both of these cases. Thus, agreement is good both qualitatively and semi-quantitatively in the cases shown here. We conclude that the theory presented is correctly predicting the magnitudes of these shear modulus enhancements resulting from pore-fluid effects.

6 SYNOPSIS AND CONCLUSIONS

The preceding discussion shows how overall shear modulus dependence on pore-fluid mechanics arises in simple anisotropic (the specific example used was transversely isotropic) media. The results (both the product formula derived previously by the author and the new formulae such as eq. 35) demonstrate in a wholly elementary fashion how compression-to-shear coupling enters the analysis for anisotropic materials and, furthermore, how this coupling leads to overall shear dependence on the mechanics of fluids in the pore system.

These effects need not always be large. However, the effect can be very substantial (on the order of a 10 to 20 per cent increase in the overall shear modulus) in cracked or fractured materials, when these pores are liquid filled. Then, the anisotropy and liquid stiffening effects both come strongly into play in the results, such as those illustrated in Figs 1–4. In particular, if $\beta_1 \simeq \beta_3$, then soft anisotropy does not make a significant contribution. However, if either $\beta_1 \ll \beta_3$ or $\beta_1 \gg \beta_3$, then the contribution can be significant.

The results presented here are expected to be useful in reconciling high-frequency shear wave data with the poroelastic theory and also as a tool for the benchmarking of poroelastic codes for complex, heterogeneous earth systems such as reservoirs.

ACKNOWLEDGMENTS

I thank W. B. Durham for a discussion of triaxial versus axisymmetric testing. Work was performed under the auspices of the US Department of Energy (DOE) under contract no. W-7405-ENG-48 and supported specifically by the Geosciences Research Program of the DOE Office of Basic Energy Sciences, Division of Chemical Sciences, Geosciences and Biosciences. Work was also supported in part by the Stanford Exploration Project, while on sabbatical visiting the Geophysics Department at Stanford University.

REFERENCES

Backus, G.E., 1962. Long-wave elastic anisotropy produced by horizontal layering, *J. geophys. Res.,* **67,** 4427–4440.

Berge, P.A. & Berryman, J.G., 1995. Realizability of negative pore compressibility in poroelastic composites, *ASME J. Appl. Mech.,* **62,** 1053–1062.

Berryman, J.G., 1999. Origin of Gassmann's equations, *Geophysics,* **64,** 1627–1629.

Berryman, J.G., 2004a. Poroelastic shear modulus dependence on pore-fluid properties arising in a model of thin isotropic layers, *Geophys. J. Int.,* **157,** 415–425.

Berryman, J.G., 2004b. Modeling high-frequency acoustic velocities in patchy and partially saturated porous rock using differential effective medium theory, *Int. J. Multiscale Computational Engineering,* **2,** 115–131.

Berryman, J.G., 2004. Bounds on elastic constants for random polycrystals of laminates, *J. Appl. Phys.,* **96**(8), 4281–4287.

Berryman, J.G., 2005. Fluid effects on shear for seismic waves in finely layered media, *Geophysics,* in press.

Berryman, J.G. & Thigpen, L., 1985. Nonlinear and semilinear dynamic poroelasticity with microstructure, *J. Mech. Phys. Solids,* **33,** 97–116.

Berryman, J.G. & Wang, H.F., 1995. The elastic coefficients of double-porosity models for fluid transport in jointed rock, *J. geophys. Res.,* **100,** 24 611–24 627.

Berryman, J.G. & Wang, H.F., 2001. Dispersion in poroelastic systems, *Phys. Rev. E,* **64,** 011303.

Berryman, J.G., Berge, P.A. & Bonner, B.P., 2002a. Estimating rock porosity and fluid saturation using only seismic velocities, *Geophysics,* **67,** 391–404.

Berryman, J.G., Pride, S.R. & Wang, H.F., 2002b. A differential scheme for elastic properties of rocks with dry or saturated cracks, *Geophys. J. Int.,* **151,** 597–611.

Biot, M.A., 1962a. Generalized theory of acoustic propagation in porous dissipative media, *J. acoust. Soc. Am.,* **34,** 1254–1264.

Biot, M.A., 1962b. Mechanics of deformation and acoustic propagation in porous media, *J. Appl. Phys.,* **33,** 1482–1498.

Biot, M.A. & Willis, D.G., 1957. The elastic coefficients of the theory of consolidation, *J. Appl. Mech.,* **24,** 594–601.

Bourbié, T., Coussy, O. & Zinszner, B., 1987. *Acoustics of Porous Media,* Gulf Publishing Company, Houston, pp. 85–95.

Brown, R.J.S. & Korringa, J., 1975. On the dependence of the elastic properties of a porous rock on the compressibility of a pore fluid, *Geophysics,* **40,** 608–616.

Chin, R.C.Y., Berryman, J.G. & Hedstrom, G.W., 1985. Generalized ray expansion for pulse propagation and attenuation in fluid-saturated porous media, *Wave Motion,* **7,** 43–66.

Gassmann, F., 1951. Über die elastizität poröser medien, *Veirteljahrsschrift der Naturforschenden Gesellschaft in Zürich,* **96,** 1–23.

Hellmich, C. & Ulm, F.-J., 2004. Micro-porodynamics of bone: Prediction of marrow pressure rises due to impact, as well as of fast, slow, and undrained wave velocities. In: *Proceedings of the 17th ASCE Engineering Mechanics Conference*, *June 13–16, 2004,* eds Kirby J. T. & Cheng A. H.-D., Paper No. 347, University of Delaware, Newark, DE.

Hudson, J.A., 1981. Wave speeds and attenuation of elastic waves in material containing cracks, *Geophys. J. R. astr. Soc.,* **64,** 133–150.

Jaeger, J.C. & Cook, N.G.W., 1976. Chapter 4: Elasticity and strength of rock, in *Fundamentals of Rock Mechanics,* pp. 77–108, Chapman and Hall, London.

Knight, R. & Nolen-Hoeksema, R., 1990. A laboratory study of the dependence of elastic wave velocities on pore scale fluid distribution, *Geophys. Res. Lett.,* **17,** 1529–1532.

Mavko, G. & Jizba, D., 1991. Estimating grain-scale fluid effects on velocity dispersion in rocks, *Geophysics,* **56,** 1940–1949.

Mukerji, T. & Mavko, G., 1994. Pore fluid effects on seismic velocity in anisotropic rocks, *Geophysics,* **59,** 233–244.

Murphy, W. F., III, 1982. Effects of Microstructure and Pore Fluids on the Acoustic Properties of Granular Sedimentary Materials, *PhD thesis,* Stanford University, Stanford, CA.

Norris, A.N., 1993. Low-frequency dispersion and attenuation in partially saturated rocks, *J. acoust. Soc. Am.,* **94,** 359–370.

O'Connell, R.J. & Budiansky, B., 1974. Seismic velocities in dry and saturated cracked solids, *J. geophys. Res.,* **79,** 5412–5426.

Paterson, M.S., 1978. Chapter 2: Experimental procedures, in *Experimental Rock Deformation—The Brittle Field,* pp. 4–15, Springer-Verlag, Berlin.

Plona, T.J., 1980. Observation of a second bulk compressional wave in a porous medium at ultrasonic frequencies, *Appl. Phys. Lett.,* **36,** 259–261.

Pride, S.R., Berryman, J.G. & Harris, J.M., 2004. Seismic attenuation due to wave induced flow, *J. geophys. Res.,* **109,** B01201.

Rice, J.R. & Cleary, M.P., 1976. Some basic stress diffusion solutions for fluid-saturated elastic porous media with compressible constituents, *Rev. Geophys.,* **14,** 227–241.

Sams, M.S., Neep, J.P., Worthington, M.H. & King, M.S., 1997. The measurement of velocity dispersion and frequency-dependent intrinsic attenuation in sedimentary rocks, *Geophysics,* **62,** 1456–1464.

Skempton, A.W., 1954. The pore-pressure coefficients *A* and *B*, *Geotechnique,* **4,** 143–147.

Walsh, J.B., 1969. New analysis of attenuation in partially melted rock, *J. geophys. Res.,* **74,** 4333–4337.

Williams, K.L., Jackson, D.R., Thorsos, E.I., Tang, D. & Schock, S.G., 2002. Comparison of sound speed and attenuation measured in a sandy sediment to predictions based on the Biot theory of porous media, *IEEE J. Ocean. Eng.,* **27,** 413–428.

Zimmerman, R.W., 1991. Chapter 7: Introduction to poroelasticity theory, in *Compressiblity of Sandstones,* pp. 66–77, Elsevier, Amsterdam.

APPENDIX A: TRIAXIAL VERSUS UNIAXIAL STRESS/STRAIN

Because a strain of the form $v_3^T = (1, 1, -2)$ (as defined in eq. 12) is clearly volume preserving, it is one type of shear strain. Furthermore, because this mode plays a key role in our analysis, we call it uniaxial shear. We also use the same term when the shear state of interest is an applied stress with the principal stress components proportional to $v_3^T = (1, 1, -2)$.

To see why this terminology might be appropriate, consider two definitions of stress appropriate to triaxial tests (see Jaeger & Cook 1976; Paterson 1978; Zimmerman 1991) :

$$\sigma_c \equiv (\sigma_{11} + \sigma_{22} + \sigma_{33})/3 \tag{A1}$$

and, most importantly,

$$q = \sigma_{33} - (\sigma_{11} + \sigma_{22})/2. \tag{A2}$$

Eq. (A1) is a definition of the average confining stress, while eq. (A2) is related in general to the shear stress. Using the definitions in eq. (12) as a basis for the principal stresses, we have

$$\begin{pmatrix} \sigma_{11} \\ \sigma_{22} \\ \sigma_{33} \end{pmatrix} = \sigma_c v_1 + a v_2 + b v_3. \tag{A3}$$

So, $\sigma_{11} = \sigma_c + a + b$, $\sigma_{22} = \sigma_c - a + b$ and $\sigma_{33} = \sigma_c - 2b$, and, therefore, for the polyaxial case we have

$$q = -3b, \tag{A4}$$

where b is the coefficient of v_3. In the typical triaxial (or perhaps a better term is axisymmetric) experiment, it is assumed that the intermediate stress $\sigma_{22} = \sigma_{11}$, which also implies that $a = 0$. However, this condition does not change the result (A4). Triaxial testing has been developed especially to study failure in rock and soil, which can depend strongly on both the hydrostatic and shear components of the stress. It clearly makes use of a superposition of hydrostatic pressure and uniaxial stress.

In our context, the term uniaxial shear refers either to a shear stress proportional to v_3 and, therefore, orthogonal to a hydrostatic stress state, or to a shear strain proportional to v_3 that is orthogonal to uniform strain in all directions. If a pure uniaxial stress or strain of magnitude 3 units is applied in direction 3, then we have

$$\begin{pmatrix} 0 \\ 0 \\ 3 \end{pmatrix} = \begin{pmatrix} 1 \\ 1 \\ 1 \end{pmatrix} - \begin{pmatrix} 1 \\ 1 \\ -2 \end{pmatrix}. \tag{A5}$$

Thus, a pure uniaxial stress or strain is the difference of a pure hydrostatic component v_1 and shear component v_3. It therefore seems natural to call this shear component the uniaxial shear. Although clearly related to the triaxial test, this concept was developed mostly as a theoretical one, convenient for distinguishing that part of the shear energy that can be coupled to externally applied hydrostatic compression or tension in a transversely isotropic (hexagonal symmetry) poroelastic system and vice versa. The same concept is also useful for some other important symmetry classes such as trigonal, tetragonal and cubic.

APPENDIX B: ENERGY ELLIPSES

The equation of an ellipse centred at the origin whose semi-major and semi-minor axes are of lengths a and b, and whose angle of rotation with respect to the x-axis in the (x, y) plane is ψ is given by

$$(x\cos\psi + y\sin\psi)^2/a^2 + (-x\sin\psi + y\cos\psi)^2/b^2 = 1. \tag{B1}$$

For comparison, when $x = r\cos\theta$, $y = r\sin\theta$ and a stress of magnitude $r = \sqrt{x^2 + y^2}$ is applied to a poroelastic system, the energy stored in the anisotropic media of interest here (using eqs 16 and 18) is given by

$$\begin{aligned} r^2 f^T(\theta)\Sigma^* f(\theta) &\equiv U(r, \theta) \\ &= 3r^2\left(A_{11}\cos^2\theta + 2\sqrt{2}A_{13}\cos\theta\sin\theta + 2A_{33}\sin^2\theta\right) \\ &= R^2 U(r_0, \theta). \end{aligned} \tag{B2}$$

In the second equation, $R \equiv r/r_0$ and r_0 is an arbitrary number (say unity) having the dimensions of stress (i.e. dimensions of Pa). It is not hard to see that, when $U(r, \theta) = \text{const}$, the two eqs (B1) and (B2) have the same functional form and, therefore, that contours of constant energy in the complex $(z = x + iy)$ plane are ellipses. Furthermore, we can solve for the parameters of the ellipse by setting $U = 1$ (in arbitrary units for now) in eq. (B2) and then factoring r^2 out of both equations. We find that

$$\begin{aligned} 3A_{11} &= \frac{\cos^2\psi}{a^2} + \frac{\sin^2\psi}{b^2}, \\ 6\sqrt{2}A_{13} &= \sin 2\psi\left(\frac{1}{a^2} - \frac{1}{b^2}\right), \\ 6A_{33} &= \frac{\sin^2\psi}{a^2} + \frac{\cos^2\psi}{b^2}. \end{aligned} \tag{B3}$$

These three equations can be inverted for the parameters of the ellipse, giving

$$\begin{aligned} \frac{1}{a^2} &= \frac{3A_{11}\cos^2\psi - 6A_{33}\sin^2\psi}{\cos 2\psi}, \\ \frac{1}{b^2} &= -\frac{3A_{11}\sin^2\psi - 6A_{33}\cos^2\psi}{\cos 2\psi}, \\ \tan 2\psi &= \frac{2\sqrt{2}A_{13}}{A_{11} - 2A_{33}}. \end{aligned} \tag{B4}$$

Although contours of constant energy are of some interest, it is probably more useful to our intuition fporoelastic application to think instead about contours associated with applied stresses and strains of unit magnitude, i.e. for $r = 1$ (in appropriate units) and θ varying from 0 to π (again see definition 18). We then have the important function $U(1, \theta)$. (Note that, when θ varies instead between

π and 2π, we just get a copy of the behaviour for θ between 0 and π. The only difference is that the stress and strain vectors have an overall minus sign relative to those on the other half-circle. For a linear system, such an overall phase factor of unit magnitude is irrelevant to the mechanics of the problem.) Then, if we set $U(r, \theta) = \text{const} = R^2\, U(r_0, \theta)$ and plot $z = Re^{i\theta}$ in the complex plane, we will have a plot of the ellipse of interest with R determined analytically by

$$R = \sqrt{U(r, \theta)/U(r_0, \theta)} = \sqrt{\text{const}/U(r_0, \theta)}. \tag{B5}$$

We call R the magnitude of the normalized stress (i.e. normalized with respect to r_0).

The analysis just outlined can then be repeated for the stiffness matrix and applied strain vectors. The mathematics is completely analogous to the case already discussed, so we will not repeat it here. Because strain is already a dimensionless quantity, the factor that plays the same role as r_0 above can in this case be chosen to be unity if desired, as the main purpose of the factor r_0 above was to keep track of the dimensions of the stress components.